ISPRS Journal of Photogrammetry and Remote Sensing 66 (2011) 700–707

Contents lists available at ScienceDirect

ISPRS Journal of Photogrammetry and Remote Sensing

journal homepage: www.elsevier.com/locate/isprsjprs

Relative orientation based on multi-features

Yongjun Zhang [a,b,*], Binghua Hu [a], Jianqing Zhang [a,b]

[a] *School of Remote Sensing and Information Engineering, Wuhan University, No. 129 Luoyu Road, Wuhan 430079, PR China*
[b] *State Key Laboratory of Information Engineering in Surveying, Mapping and Remote Sensing, No. 129 Luoyu Road, Wuhan 430079, PR China*

ARTICLE INFO

Article history:
Received 5 June 2010
Received in revised form 21 May 2011
Accepted 1 June 2011
Available online 6 July 2011

Keywords:
Multi-features
Straight line
Circular curve
Relative orientation
Precision analysis

ABSTRACT

In digital photogrammetry, corresponding points have been widely used as the basic source of information to determine the relative orientation parameters among adjacent images. Sometimes, though, the conventional relative orientation process cannot be precisely implemented due to the accumulation of random errors or in the case of inadequate corresponding points. A new relative orientation approach with multiple types of corresponding features, including points, straight lines, and circular curves, is proposed in this paper. The origin of the model coordinate system is set at the projection center of the first image of a strip, and all of the exterior orientation parameters, except φ and ω of the first image, are set at zero. The basic models of relative orientation with corresponding points, straight lines, and circular curves are discussed, and the general form of a least squares adjustment model for relative orientation based on multi-features is established. Our experimental results show that the proposed approach is feasible and can achieve more reliable relative orientation results than the conventional approach based on corresponding points only.

1. Introduction

Relative orientation is one of the most important procedures in photogrammetry. It is traditionally implemented using a group of well-defined corresponding points (Tang and Heipke, 1996; Zhang, 1998; Stewénius et al., 2006). However, with the ever-expanding applications of photogrammetric technology, the conventional procedure for relative orientation is unable to fulfill the requirements of various applications (Habib and Kelley, 2001). More features, besides points, are necessary in order to perform relative orientation and subsequent procedures (Heuvel, 1997, 1998; Smith and Park, 2000; Nistér, 2004). Schenk (2004) proposed a novel model of feature-based aerial triangulation. Habib et al. (2004) discussed the applications of linear features in photogrammetric activities, such as resection, triangulation, image to image registration and surface to surface registration. A model of generalized point photogrammetry (Zhang et al., 2008) was proposed which uses more geometric features such as straight lines and circular curves in photogrammetric applications. This model has been successfully used in the areas of three-dimensional urban modeling, industrial photogrammetry, and determination of the aircraft attitudes.

In order to overcome the disadvantages of the conventional relative orientation approach, such as the accumulation of random errors, linear features have been used in relative orientation (Heuvel, 1997; Habib, 1999; Smith and Park, 2000; Habib and Kelley, 2001; Battha, 2004). It is easier to automatically extract linear features than distinct points from imagery. In addition, images covering areas with man-made objects are usually rich in linear features (Tommaselli and Lugnani, 1988; Kubik, 1991). Moreover, in the process of constructing a single strip free network using conventional relative orientation based on feature points only, the strip is likely to be bended due to the accumulation of random errors. However, relative orientation based on linear and curved features other than feature points can significantly reduce the strip bending problem owing to the geometric constraints between these features. They can be incorporated into the mathematical adjustment model of relative orientation so that the redundancy can be increased and the geometric stability can be enhanced (Habib et al., 2004).

Relative pose estimation is also an important topic in computer vision communities. A new algorithm on computing the three-dimensional path of a moving rigid object was proposed by Laganière et al. (2006) using a pre-calibrated stereoscopic vision instrument. Rahmann and Dikov (2008) proposed a linear approach of relative orientation using two arbitrary circles. An algorithm of automatic detection of a chessboard for camera calibration and pose estimation with one circle as a probe was proposed by Ha (2009). Wang et al. (2008) proved that the camera pose of an image can be uniquely recovered with one circle or two general pairs of parallel lines under certain assumptions. Bundle-adjusted camera and scene-feature positions were used by Warren et al. (2010) for dense 3D reconstructions of large scale environments from UAV images.

* Corresponding author at: School of Remote Sensing and Information Engineering, Wuhan University, No. 129 Luoyu Road, Wuhan 430079, PR China.
E-mail address: zhangyj@whu.edu.cn (Y. Zhang).

0924-2716/$ - see front matter © 2011 International Society for Photogrammetry and Remote Sensing, Inc. (ISPRS). Published by Elsevier B.V. All rights reserved.
doi:10.1016/j.isprsjprs.2011.06.001

A new relative orientation approach based on multiple types of corresponding image features (i.e., straight lines, circles, and points) is proposed in this paper. The mathematical model of relative orientation with multi-features is discussed in Section 2. Several experiments are performed to verify the correctness and to evaluate the performance of the proposed approach in Section 3. Finally, conclusions are presented and future work is outlined.

2. Mathematical model of relative orientation with multi-features

Relative orientation is the process of determining the relative baseline vector of two perspective centers and the relative rotation angles of one image against the other of a stereo, which totally consists of only five parameters if the camera interior elements are known (Pan, 1999). The five parameters can be determined in several ways, such as dependent relative orientation and independent relative orientation (Mikhail et al., 2001). In this paper, the dependent relative orientation strategy is chosen and thus the relative orientation parameters are $\varphi, \omega, \kappa, \mu, v$ (Habib and Kelley, 2001), where φ, ω, κ are the rotation angles and μ, v the baseline parameters of the right image of a stereo pair. The baseline length Bx is usually selected as the mean x-parallax of corresponding features, and $By = Bx \cdot \mu, Bz = Bx \cdot v$.

In this paper, the origin of the model coordinate system is set to be the projection center of the first image of a strip, the Z-axis of the model coordinate system is set to be in parallel with that of the world coordinate system, the X-axis is set to be the same as the X-axis of the image coordinate system of the first image, and the Y-axis is set to be perpendicular to both the X-axis and Z-axis to form a right-hand rectangular coordinate system. Therefore, the exterior orientation parameters of the first image of a strip under the model coordinate system should be (0, 0, 0, φ, ω, 0).

2.1. Model of relative orientation with straight line

A stereo pair is depicted in Fig. 1 with an object line l, two corresponding image lines ab and cd, and two perspective centers S_1 and S_2. Let P_1 denote the plane defined by points S_1, a and b; let P_2 denote the plane defined by points S_2, c and d; and let $n_1(A, B, C)$ and $n_2(A', B', C')$ denote the normal vectors of P_1 and P_2, respectively. Plane P_1 should intersect plane P_2 at the object straight line l. The direction vector of the line l should be $n(BC' - B'C, A'C - AC', AB' - A'B)$ according to the intersection of two planes.

Hence, if line l is a horizontal line,

$$AB' - A'B = 0 \tag{1}$$

and if line l is a vertical line,

$$BC' - B'C = 0, \quad AC' - A'C = 0 \tag{2}$$

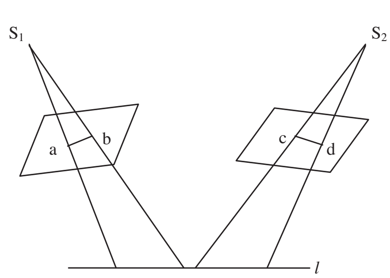

Fig. 1. Relative orientation with straight lines.

Based on the theory of planar vector, the following two equations can be obtained:

$$n_1(A, B, C) = \begin{vmatrix} i & j & k \\ X_1 & Y_1 & Z_1 \\ X_2 & Y_2 & Z_2 \end{vmatrix} = (Y_1Z_2 - Y_2Z_1, X_2Z_1 - X_1Z_2, X_1Y_2 - X_2Y_1) \tag{3}$$

$$n_2(A', B', C') = \begin{vmatrix} i & j & k \\ X_3 & Y_3 & Z_3 \\ X_4 & Y_4 & Z_4 \end{vmatrix} = (Y_3Z_4 - Y_4Z_3, X_4Z_3 - X_3Z_4, X_3Y_4 - X_4Y_3) \tag{4}$$

When Eqs. (3) and (4) are substituted into Eq. (1), Eq. (1) becomes

$$F_1 = (Y_1Z_2 - Y_2Z_1)(X_4Z_3 - X_3Z_4) - (Y_3Z_4 - Y_4Z_3)(X_2Z_1 - X_1Z_2) = 0 \tag{5}$$

Similarly, Eq. (2) becomes

$$F_2 = (X_2Z_1 - X_1Z_2)(X_3Y_4 - X_4Y_3) - (X_4Z_3 - X_3Z_4)(X_1Y_2 - X_2Y_1) = 0 \tag{6}$$

$$F_3 = (Y_1Z_2 - Y_2Z_1)(X_3Y_4 - X_4Y_3) - (Y_3Z_4 - Y_4Z_3)(X_1Y_2 - X_2Y_1) = 0 \tag{7}$$

where (X_1, Y_1, Z_1), (X_2, Y_2, Z_2), (X_3, Y_3, Z_3) and (X_4, Y_4, Z_4) denote the spatial auxiliary coordinates of the points a, b, c and d, which can be calculated by the following equation.

$$\begin{bmatrix} X \\ Y \\ Z \end{bmatrix} = R \begin{bmatrix} x \\ y \\ -f \end{bmatrix} \tag{8}$$

where $R = \begin{pmatrix} \cos\varphi\cos\kappa - \sin\kappa\sin\omega\sin\kappa & -\cos\varphi\sin\kappa - \sin\varphi\sin\omega\cos\kappa & -\sin\varphi\cos\omega \\ \cos\omega\sin\kappa & \cos\omega\cos\kappa & -\sin\omega \\ \sin\varphi\cos\kappa + \cos\varphi\sin\omega\sin\kappa & -\sin\varphi\sin\kappa + \cos\varphi\sin\omega\cos\kappa & \cos\varphi\cos\omega \end{pmatrix}$, φ, ω, κ the three rotation angles taking the Y axis as the primary axis, (X, Y, Z) the spatial auxiliary coordinates of a certain point with image coordinate (x, y), f the focal length of the camera.

Eqs. (5)–(7) of corresponding lines can be used for relative orientation instead of the conventional coplanarity equation used by corresponding points. Because (X_1, Y_1, Z_1) and (X_2, Y_2, Z_2) are known, (X_3, Y_3, Z_3) and (X_4, Y_4, Z_4) are functions of independent parameters φ, ω, κ and μ, v, Eqs. (5)–(7) can be linearized according to the Taylor series, so that three equations with the following forms can be obtained:

$$\begin{aligned} F_1 = F_1^0 &+ (X_1Z_2 - X_2Z_1)(X_4Y_3 - X_3Y_4)d\varphi \\ &+ (Y_1Z_2 - Y_2Z_1)(X_4Y_3 - X_3Y_4)d\omega + ((Y_1Z_2 - Y_2Z_1)(Y_3Z_4 - Y_4Z_3) \\ &+ (X_1Z_2 - X_2Z_1)(X_3Z_4 - X_4Z_3))d\kappa = 0 \end{aligned} \tag{9}$$

$$\begin{aligned} F_2 = F_2^0 &+ (X_2Z_1 - X_1Z_2)(Y_3Z_4 - Y_4Z_3)d\varphi \\ &+ ((X_1Z_2 - X_2Z_1)(X_3Z_4 - X_4Z_3) + (X_1Y_2 - X_2Y_1)(X_3Y_4 - X_4Y_3))d\omega \\ &- (X_1Y_2 - X_2Y_1)(Y_3Z_4 - Y_4Z_3)d\kappa = 0 \end{aligned} \tag{10}$$

$$\begin{aligned} F_3 = F_3^0 &+ ((Y_1Z_2 - Y_2Z_1)(Y_3Z_4 - Y_4Z_3) \\ &+ (X_1Y_2 - X_2Y_1)(X_3Y_4 - X_4Y_3))d\varphi - (Y_1Z_2 - Y_2Z_1)(X_3Z_4 - X_4Z_3)d\omega \\ &- (X_1Y_2 - X_2Y_1)(X_3Z_4 - X_4Z_3)d\kappa = 0 \end{aligned} \tag{11}$$

where $F_i^0 (i = 1, 2, 3)$ is the approximate value of F_i which can be calculated according to the corresponding equation using the approximations of the relative orientation parameters, $d\varphi, d\omega, d\kappa$ are corrections to the angular parameters of relative orientation.

Since the above equations contain angular parameters only, at least two corresponding points are necessary to solve the five relative orientation parameters.

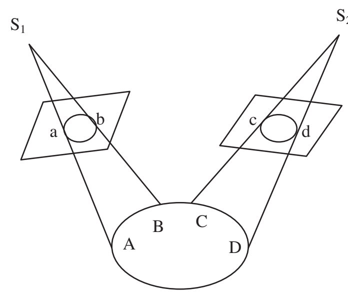

Fig. 2. Relative orientation with circular curves.

2.2. Model of relative orientation with a circle

Given a stereo pair, as depicted in Fig. 2, it contains an object circle, two corresponding image circles, and two perspective centers S_1 and S_2. Two vectors from S_1 intersect the left image circle at points a and b and intersect the object circle at points A and B. Another two vectors from S_2 intersect the right image circle at points c and d, and intersect the object circle at points C and D. Here, we assume that the model coordinates of the four object points A, B, C, and D are (Xp_1, Yp_1, Zp_1), (Xp_2, Yp_2, Zp_2), (Xp_3, Yp_3, Zp_3) and (Xp_4, Yp_4, Zp_4), respectively. Suppose that the object circle lies in a horizontal plane with a certain height Zp. Assuming the model coordinates of the circle center being (X_0, Y_0, Zp) and the circle radius being R, we obtain the following two equations:

$$Zp_1 = Zp_2 = Zp_3 = Zp_4 = Zp \tag{12}$$

$$(Xp_i - X_0)^2 + (Yp_i - Y_0)^2 = R^2, \quad (i = 1,2,3,4) \tag{13}$$

According to Eq. (13), the relationship between the coordinates of the circles in the left and right images can be obtained and the error equations can be established. Then, it is possible to solve the relative orientation parameters by least square adjustment.

Assuming that the exterior orientation parameters of the left image are known with the translation parameters being Xs_1, Ys_1, and Zs_1, the rotation parameters being φ_0, ω_0, and κ_0, and the unknown translation parameters of the right image being Xs_2, Ys_2, and Zs_2, the rotation parameters are φ, ω, and κ, then the components of the baseline can be calculated as follows:

$$Bx = Xs_2 - Xs_1, \quad By = Ys_2 - Ys_1 = \mu Bx, \quad Bz = Zs_2 - Zs_1 = vBx \tag{14}$$

The model coordinates of the circle center can be calculated by forward intersection as following:

$$\begin{aligned} &N = \tfrac{Bx(Z_{02} - vX_{02})}{X_{01}Z_{02} - Z_{01}X_{02}} \quad N' = \tfrac{Bx(Z_{01} - vX_{01})}{X_{01}Z_{02} - Z_{01}X_{02}} \\ &X_0 = Xs_1 + Bx + N'X_{02} \quad Zp = Zs_1 + vBx + N'Z_{02} \\ &Y_0 = Ys_1 + \mu Bx + N'Y_{02} = Ys_1 + \tfrac{1}{2}(NY_{01} + N'Y_{02} + \mu Bx) \end{aligned} \tag{15}$$

where (X_{01}, Y_{01}, Z_{01}) and (X_{02}, Y_{02}, Z_{02}) are the spatial auxiliary coordinates of the corresponding points of the object circle center in the left and right images, N and N' are the point projection coefficients of the left and right circle centers, μ, v are the baseline components.

The points S_1, a and A of the left image are collinear so we can obtain the following equation:

$$(X_1, Y_1, Z_1) = k_1(Xp_1 - Xs_1, Yp_1 - Ys_1, Zp - Zs_1) \tag{16}$$

then

$$Xp_1 = X_1(Zp - Zs_1)/Z_1 + Xs_1, \quad Yp_1 = Y_1(Zp - Zs_1)/Z_1 + Ys_1 \tag{17}$$

Substituting Eq. (17) into Eq. (13), the following equation can be obtained:

$$\left(\frac{X_1}{Z_1}(Zp - Zs_1) + Xs_1 - X_0\right)^2 + \left(\frac{Y_1}{Z_1}(Zp - Zs_1) + Ys_1 - Y_0\right)^2 - R^2 = 0 \tag{18}$$

Similarly, points S_2, c and C of the right image are also collinear. We obtained the following equation:

$$\left(\frac{X_3}{Z_3}(Zp - Zs_2) + Xs_2 - X_0\right)^2 + \left(\frac{Y_3}{Z_3}(Zp - Zs_2) + Ys_2 - Y_0\right)^2 - R^2 = 0 \tag{19}$$

where (X_1, Y_1, Z_1) and (X_3, Y_3, Z_3) are the spatial auxiliary coordinates of points a and c, respectively.

According to Eqs. (18) and (19), the relationship between the two images can be established as follows:

$$\begin{aligned} F = &\left(\frac{X_1}{Z_1}(Zp - Zs_1) + Xs_1 - X_0\right)^2 + \left(\frac{Y_1}{Z_1}(Zp - Zs_1) + Ys_1 - Y_0\right)^2 \\ &- \left(\frac{X_3}{Z_3}(Zp - Zs_2) + Xs_2 - X_0\right)^2 \\ &- \left(\frac{Y_3}{Z_3}(Zp - Zs_2) + Ys_2 - Y_0\right)^2 = 0 \end{aligned} \tag{20}$$

Substituting Eqs. (14) and (15) into Eq. (20) and expanding it according to Taylor series, linearized error equation with the following form can be obtained:

$$F = F_0 + \frac{\partial F}{\partial \varphi}d\varphi + \frac{\partial F}{\partial \omega}d\omega + \frac{\partial F}{\partial \kappa}d\kappa + \frac{\partial F}{\partial \mu}d\mu + \frac{\partial F}{\partial v}dv = 0 \tag{21}$$

Different circles have different parameters (X_0, Y_0, Zp), so (X_0, Y_0, Zp) are expressed by the relative orientation parameters and spatial auxiliary coordinates of image points corresponding to the object circle center using forward intersection in order to avoid too many additional parameters. Consequently, when calculating the partial derivatives of F with respect to the five relative orientation parameters, the partial derivatives of X_0, Y_0 and Zp with respect to the parameters should also be calculated.

During implementation, the image coordinates of the projected circle center are obtained by using more than three image points to fit an ellipse. Note that the spatial auxiliary coordinates of the circle center should be recalculated in iterations which are similar to the calculation of the spatial auxiliary coordinates of the corresponding points in the right image.

As we know, more observations could increase the redundancy and thus ensure the stability and reliability of photogrammetric adjustments (Triggs et al., 2000). Similar to points a and c, b and d, all other point pairs on the circle can also be used to establish the error equation in the form of Eq. (21).

2.3. Conventional model of relative orientation with point

According to the coplanarity condition that the two perspective centers and two corresponding image rays lie in the same plane (Mikhail et al., 2001), we could obtain the mathematical model of conventional relative orientation:

$$q + \frac{X_2Y_2}{Z_2}N'd\varphi + \left(Z_2 + \frac{Y_2^2}{Z_2}\right)N'd\omega - X_2N'd\kappa - Bxd\mu + \frac{Y_2}{Z_2}Bxdv = 0 \tag{22}$$

$$q = NY_1 - N'Y_2 - \mu B_X \tag{23}$$

where, q is the y-parallax of relative orientation, (X_1, Y_1, Z_1) and (X_2, Y_2, Z_2) the spatial auxiliary coordinates of corresponding image points respectively, N and N' the point projection coefficients of the point pair, and $d\varphi, d\omega, d\kappa, d\mu, dv$ the corrections of the relative orientation parameters.

2.4. General model of relative orientation with multi-features

According to the mathematical models of relative orientation based on corresponding straight lines, circles, and points, it is easy to establish the combined adjustment model of relative orientation based on multi-features in the following matrix form:

$$V = BX - L, \quad P \tag{24}$$

where $V = \begin{bmatrix} V_{point} \\ V_{lline} \\ V_{vline} \\ V_{circle} \end{bmatrix}$, $B = \begin{bmatrix} B_{point} \\ B_{lline} \\ B_{vline} \\ B_{circle} \end{bmatrix}$, $L = \begin{bmatrix} L_{point} \\ L_{lline} \\ L_{vline} \\ L_{circle} \end{bmatrix}$, $P = diag \begin{bmatrix} P_{point} \\ P_{lline} \\ P_{vline} \\ P_{circle} \end{bmatrix}$, X is a vector of corrections to the relative orientation parameters, $B_{point}, B_{lline}, B_{vline}$ and B_{circle} are the coefficient matrixes of the error equations established based on the corresponding points, horizontal lines, vertical lines, and circular curves, respectively, L_{point}, L_{lline}, L_{vline} and L_{circle} are constant items of the corresponding features which can be calculated by observations and the approximations of the unknowns, $P_{point}, P_{lline}, P_{vline}$ and P_{circle} are the weight matrixes of the corresponding observations.

In the process of solving the relative orientation parameters, the above weight matrixes can be determined according to the accuracy, reliability and the number of redundant observations of each type of features. If the accuracy of the lines and circles is higher and the number of redundant observations is less than those of points, the weights of these two kinds of features should be larger than that of the points in order to overcome the strip deformation problem; otherwise, the strip may deforms significantly. Therefore, it is important to select approximate weights for all features in order to achieve a better relative orientation result.

Additionally, when constructing the free network of strips, using zero as the approximate values of the angular elements of the first image may lead to a bad relative orientation result if their true values are not close to zero. Therefore, it is first necessary to calculate the rotation angle of the first image as follows: (1) measure a certain number of vertical lines in the image and calculate the coordinates of the image nadir point by least squares adjustment; (2) let the angle $\kappa = 0$, then calculate the values of φ and ω using anti-transform of the formula used to calculate the image nadir point coordinates (Heuvel, 1998). Since the nadir point constraint is utilized, the angular parameters of the first image are already spatially recovered. Therefore, due to the geometric constraints of the features, such as horizontal lines and vertical lines, the total strip is expected to be approximately horizontal also after all of the images are relatively orientated, although there may be some errors in the observations.

3. Experiments and discussions

The correctness and performance of the proposed relative orientation approach will be tested with a set of digital low-altitude images. All images are taken by a pre-calibrated Kodak Pro SLR digital camera with 4500 pixels $\times$ 3000 pixels image format and 0.008 mm physical pixel size. The focal length of the camera is 24.3355 mm. Four experiments are performed to evaluate the proposed approach. The initial values of all the relative orientation parameters in each experiment are set to be zero.

In the first experiment, three corresponding horizontal lines, three corresponding vertical lines, and ten corresponding points obtained from a stereo pair at the middle of a strip are used to verify the correctness and feasibility of the proposed model of relative orientation with straight lines. The known rotation angles of the left image are $\varphi_0 = 0.006330$ rad, $\omega_0 = -0.094454$ rad, and $\kappa_0 = 0.284277$ rad, respectively. In the second experiment, the test data containing four corresponding image circles and nine corresponding points obtained from a stereo pair at the end of a strip are used to verify the correctness and feasibility of the proposed model of relative orientation with circular curves. The known rotation angles of the left image are $\varphi_0 = 0.011419$ rad, $\omega_0 = -0.039956$ rad, and $\kappa_0 = 0.286259$ rad, respectively. In the third experiment, there are three corresponding horizontal lines, three corresponding vertical lines, four corresponding circles, and

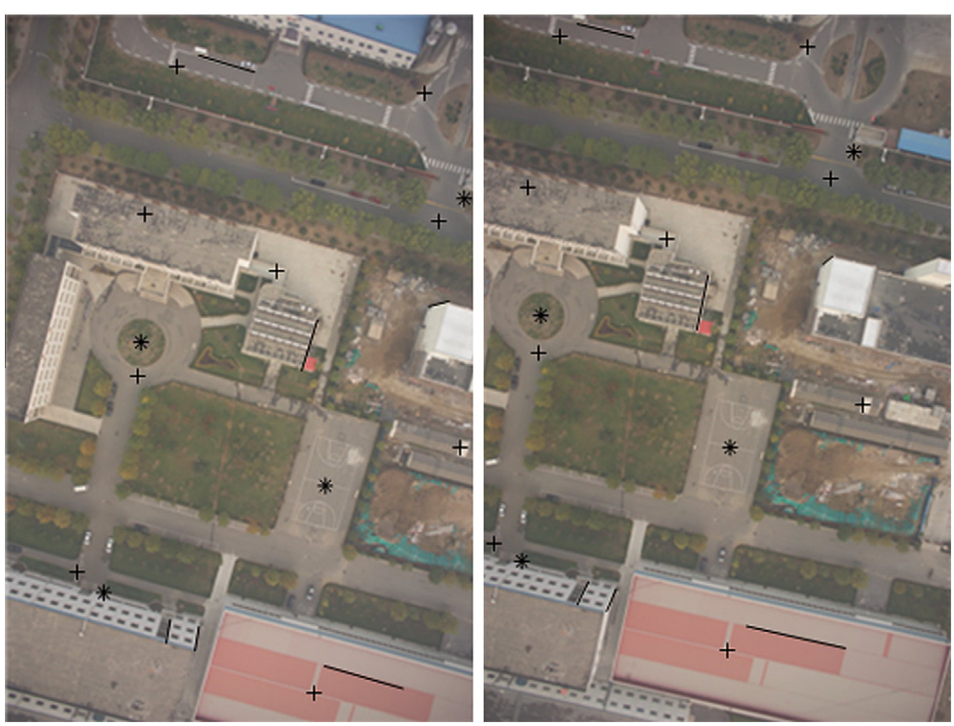

Fig. 3. The distribution of corresponding features of a stereo pair. Lines are corresponding horizontal and vertical lines, stars are the centers of corresponding circles, and crosses are corresponding points.

Table 1
Results of relative orientation obtained by corresponding straight lines and points with different approaches.

Strategy of relative orientation	Test data (the number of horizontal lines, vertical lines, points)	Results of relative orientation (rad/dimensionless)	Precision		Times of iterations
			RMSE of unit weight (mm)	RMSE of unknown parameters (rad/dimensionless)	
Conventional relative orientation	(0, 0, 10)	$\varphi = 0.047072$ $\omega = -0.105888$ $\kappa = 0.268811$ $\mu = 0.100167$ $\nu = -0.032009$	0.001534	0.000132 0.000088 0.000062 0.000587 0.000246	6
The proposed approach	(3, 3, 10)	$\varphi = 0.047071$ $\omega = -0.105890$ $\kappa = 0.268798$ $\mu = 0.100195$ $\nu = -0.032015$	0.001211	0.000104 0.000070 0.000049 0.000464 0.000194	5
	(3, 0, 4)	$\varphi = 0.048222$ $\omega = -0.105458$ $\kappa = 0.268035$ $\mu = 0.098993$ $\nu = -0.035023$	0.003586	0.000834 0.000509 0.000360 0.003069 0.001793	5
	(0, 3, 4)	$\varphi = 0.047952$ $\omega = -0.105610$ $\kappa = 0.268247$ $\mu = 0.099660$ $\nu = -0.034303$	0.002366	0.000839 0.000404 0.000399 0.002202 0.001912	5
	(3, 3, 4)	$\varphi = 0.048171$ $\omega = -0.105468$ $\kappa = 0.268017$ $\mu = 0.099005$ $\nu = -0.035008$	0.002373	0.000437 0.000303 0.000187 0.001907 0.000940	5

Table 2
Results of relative orientation obtained by corresponding circles and points.

Strategy of relative orientation	Test data (number of circles, points)	Results of relative orientation (rad/ dimensionless)	Precision		Times of iterations
			RMSE of unit weight (mm)	RMSE of unknown parameters (rad/ dimensionless)	
Conventional relative orientation	(0, 9)	$\varphi = -0.000108$ $\omega = -0.070919$ $\kappa = 0.235705$ $\mu = 0.019486$ $\nu = 0.036702$	0.001109	0.000145 0.000098 0.000059 0.000617 0.000226	5
The proposed approach	(4, 9)	$\varphi = -0.000185$ $\omega = -0.070984$ $\kappa = 0.235727$ $\mu = 0.019867$ $\nu = 0.036744$	0.001090	0.000131 0.000089 0.000051 0.000554 0.000199	3
	(4, 1)	$\varphi = -0.000242$ $\omega = -0.071143$ $\kappa = 0.235764$ $\mu = 0.020829$ $\nu = 0.036824$	0.000958	0.000236 0.000162 0.000096 0.000983 0.000413	4

nine corresponding points obtained from the same stereo pair as the second group. The distribution of the features of the third experiment is shown in Fig. 3. Lines in Fig. 3 are corresponding horizontal and vertical lines, stars are the centers of corresponding circles, and crosses are corresponding points. They are used to verify the feasibility and advantage of the proposed approach with multiple types of features. In the last experiment, a set of corresponding horizontal lines, vertical lines, circular curves, and corresponding points are obtained from a strip with 22 images. There is no outlier in all of these observations since they are interactively checked. They are used to verify the effectiveness of the proposed relative orientation approach on reduction of the strip bending problem. In the following experiments, the unit of φ, ω and κ is radian, the unit of root mean square errors (RMSE) is millimeter, while μ and ν is dimensionless because the unit of Bx is millimeter.

3.1. Relative orientation with straight lines and points

The results of the first experiment in Table 1 show that, when compared to the conventional relative orientation approach using ten corresponding points only, the proposed relative orientation approach using three corresponding horizontal lines, three corresponding vertical lines, and ten corresponding points not only ensures the validity of relative orientation results, but also slightly improves the RMSE of both the unit weight and the unknowns. Table 1 also shows that the proposed approach based on both corresponding straight lines and corresponding points can obtain reasonable relative orientation results even in the case that not enough corresponding points are available and the conventional point-based relative orientation cannot be implemented. For example only four corresponding points are used for the last three

Table 3
Results of relative orientation obtained by corresponding straight lines, circles and points.

Strategy of relative orientation	Test data (number of horizontal lines, vertical lines, circles, points)	Results of relative orientation (rad/dimensionless)	Precision		Times of iterations
			RMSE of unit weight (mm)	RMSE of unknown parameters (rad/dimensionless)	
Conventional relative orientation	(0, 0, 0, 9)	$\varphi = -0.000108$	0.001109	0.000145	5
		$\omega = -0.070919$		0.000098	
		$\kappa = 0.235705$		0.000059	
		$\mu = 0.019486$		0.000617	
		$v = 0.036702$		0.000226	
The proposed approach	(3, 3, 4, 9)	$\varphi = -0.000152$	0.001028	0.000119	4
		$\omega = -0.070944$		0.000083	
		$\kappa = 0.235757$		0.000047	
		$\mu = 0.019602$		0.000513	
		$v = 0.036778$		0.000187	
	(3, 0, 4, 1)	$\varphi = -0.000219$	0.001424	0.000284	5
		$\omega = -0.070841$		0.000195	
		$\kappa = 0.235873$		0.000111	
		$\mu = 0.018919$		0.001177	
		$v = 0.036792$		0.000540	
	(0, 3, 4, 1)	$\varphi = -0.000177$	0.001289	0.000284	5
		$\omega = -0.070850$		0.000176	
		$\kappa = 0.235861$		0.000109	
		$\mu = 0.018961$		0.001065	
		$v = 0.036863$		0.000518	
	(3, 3, 4, 1)	$\varphi = -0.000180$	0.001251	0.000247	5
		$\omega = -0.070848$		0.000171	
		$\kappa = 0.235866$		0.000097	
		$\mu = 0.018958$		0.001034	
		$v = 0.036855$		0.000472	

Table 4
Results of single strip relative orientation obtained by points and multi-features.

Image	Conventional relative orientation with points only						Relative orientation with multi-feature					
	Translation parameters (mm) (Xs, Ys, Zs)			Rotation parameters (rad) $(\varphi, \omega, \kappa)$			Translation parameters (mm) (Xs, Ys, Zs)			Rotation parameters (rad) $(\varphi, \omega, \kappa)$		
1	0.000	0.000	0.000	0.00966	−0.08118	0.00000	0.0000	0.000	0.000	0.00966	−0.08118	0.00000
2	4.345	−1.200	−0.061	0.00077	−0.06078	−0.07855	4.345	−1.257	0.141	0.01672	−0.06232	−0.07383
3	8.502	−2.343	−0.247	−0.04123	−0.08126	−0.05758	8.502	−2.365	0.188	−0.01650	−0.08559	−0.05280
4	12.282	−3.287	−0.668	−0.07160	−0.06564	−0.00592	12.282	−3.323	0.049	−0.02230	−0.07447	0.00404
5	16.380	−4.405	−1.112	−0.06480	−0.04924	−0.07085	16.380	−4.395	−0.009	0.00069	−0.06157	−0.05654
6	21.227	−5.930	−1.647	−0.08651	−0.06641	−0.08027	21.227	−5.774	−0.005	−0.00110	−0.08684	−0.06624
7	25.488	−7.140	−2.294	−0.12400	−0.09708	−0.00577	25.488	−6.921	−0.078	−0.01280	−0.12462	0.00651
8	29.746	−8.031	−3.011	−0.11715	−0.00455	−0.09265	29.746	−7.947	−0.094	0.02971	−0.03068	−0.07527
9	34.608	−10.190	−3.872	−0.20452	−0.03251	−0.05130	34.607	−10.138	0.104	−0.03370	−0.06629	−0.04482
10	37.246	−11.056	−4.667	−0.21767	−0.06895	0.00401	37.246	−11.041	−0.111	−0.03000	−0.10417	0.00832
11	42.291	−12.259	−6.153	−0.21227	−0.05926	−0.00091	42.291	−12.357	−0.344	0.02148	−0.10011	0.00778
12	48.327	−13.406	−7.825	−0.23463	0.03671	−0.09559	48.327	−13.731	−0.222	0.03028	0.00109	−0.09056
13	52.474	−14.566	−9.063	−0.33018	−0.00937	−0.05142	52.474	−14.893	−0.077	−0.04480	−0.04749	−0.06435
14	55.079	−15.391	−10.161	−0.35132	−0.03549	0.01400	55.079	−15.659	−0.235	−0.03110	−0.08670	−0.00032
15	59.579	−16.227	−12.264	−0.34403	0.00072	−0.02871	59.579	−16.894	−0.524	0.01959	−0.04575	−0.04030
16	64.959	−17.575	−14.835	−0.37893	0.02174	−0.07239	64.959	−18.232	−0.728	0.00790	−0.02882	−0.08747
17	69.429	−18.611	−17.451	−0.45456	−0.01527	−0.03294	69.429	−19.586	−0.871	−0.00660	−0.06693	−0.06977
18	71.718	−19.241	−18.754	−0.43060	−0.05376	−0.00036	71.718	−20.158	−0.946	0.00510	−0.10530	−0.02199
19	75.629	−20.274	−20.941	−0.36981	0.01703	−0.04603	75.629	−21.217	−0.943	0.05332	−0.02853	−0.04105
20	81.974	−22.392	−23.586	−0.43237	−0.03062	−0.04614	81.974	−23.210	−0.609	0.02102	−0.08393	−0.05767
21	84.821	−23.258	−25.069	−0.44855	−0.05731	0.02285	84.821	−24.017	−0.558	0.00486	−0.11116	0.00654
22	89.184	−23.816	−27.564	−0.45254	−0.00105	−0.00068	89.184	−24.816	−0.660	0.03841	−0.05459	−0.01401

tests in Table 1, and the RMSEs of the unit weight of the five tests in Table 1 are all smaller than one-half of a pixel. So the proposed approach can somewhat solve the relative orientation problem of stereo images lacking enough corresponding points but with obvious feature lines. However, one should use as many observations as possible in order to enhance the reliability of the relative orientation in actual applications.

3.2. Relative orientation with circles and points

As shown in Table 2, the results of the second experiment indicate that the proposed mathematical model of relative orientation with circular curves and points can achieve slightly better relative orientation results with higher stability and accuracy than those obtained by the conventional approach with nine corresponding points only. As can be seen from the last test in Table 2, a satisfied relative orientation result can still be obtained by combining four corresponding circles and only one corresponding point. However, this observation does not mean that the fewer the points used, the better the results achieved. Although the RMSE of the unit weight increases while the number of observations decreases, the RMSE of the unknown parameters increases reversely. In general, the more observations utilized, the higher are the reliability and accuracy of the results.

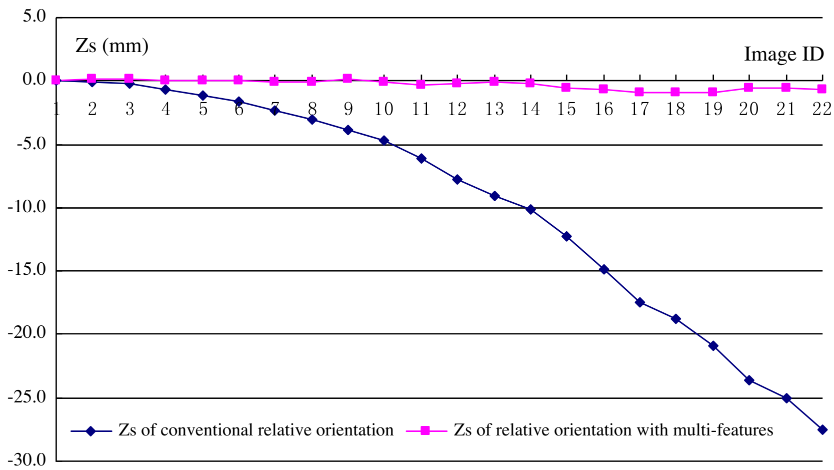

Fig. 4. Relative orientation elements Zs obtained by the two approaches.

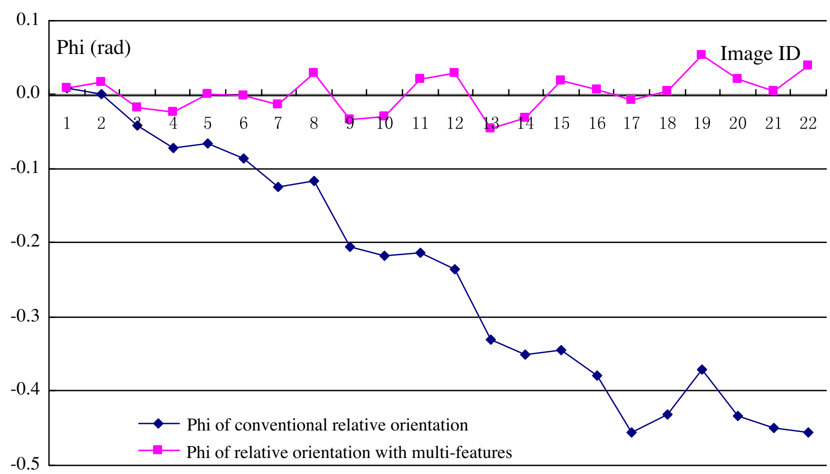

Fig. 5. Relative orientation elements Phi (φ) obtained by the two approaches.

3.3. Relative orientation with multi-features

The results of the third experiment, shown in Table 3, indicate that the proposed relative orientation approach based on multi-features is feasible and can improve the accuracy and reliability of relative orientation. Since more features are employed in relative orientation, the required number of feature points is significantly less. For example, very good relative orientation results can be obtained with three to four corresponding lines and circles and only one corresponding point. In a case where the relative orientation accuracy requirement is not very high, relative orientation can be implemented without corresponding points if there are enough evenly distributed corresponding circles and straight lines.

The relative orientation elements of each image obtained by the proposed approach and the conventional approach of the last experiment are shown in Table 4. The exterior orientation parameters of the first image are identical for both approaches. Comparisons of the achieved elements Zs and Phi (i.e., φ) of the two approaches are shown in Figs. 4 and 5, respectively. It is clear that the elements Zs and φ of the conventional approach are closely correlated. The strip is seriously bended due to the accumulation of random errors. We think that this problem is mainly caused by two reasons: the first is that only 9–10 points are used for relative orientation; and the second is that although the camera is pre-calibrated, there are still some small residuals of lens distortions. However, the proposed relative orientation approach based on multi-features can significantly reduce the strip bending problem since the leveling and vertical constraints are used to establish the mathematical model.

As mentioned in Section 2.4, the approximate weights of the observations significantly influence the results of relative orientation. In this paper, the approximate weights of the lines and circles are manually set to be 2.0, while they are 1.0 for the point observations. Actually, the achieved relative orientation results are similar when the weights of lines and circles are in the range of 1.5–3.0. However, the results worsen if the weights of the lines and circles are set smaller than 1.0 or larger than 3.0.

4. Conclusions

In this paper, the problem of conventional relative orientation was discussed and a new approach based on multi-features was proposed in this paper. The experimental results show the advantages of the new approach over the conventional method in robustness, reliability, and availability. Enhanced performance is achieved by the increased redundancy of the line and circular features, which are automatically extracted from digital imagery and combined with feature points to solve the parameters of relative orientation. By utilizing the horizontal and vertical constraints, the proposed approach can effectively reduce the strip deformation problem caused by the accumulation of random errors in the conventional relative orientation that is based solely on corresponding points. However, the proposed approach uses only horizontal straight lines, vertical straight lines, circular curves, and points so it is unsuitable for the relative orientation of stereo images with inclined straight lines and general curves, which are future work to be further investigated.

Acknowledgement

This work is supported by the National Key Technology Research and Development Program with Project No. 2011BAH12B05, the National Natural Science Foundation of China with Project No. 41071233, the National High Technology Research and Development Program with Project No. 2009AA121403, Nonprofit Special Project of Ministry of Land and Resources with Project No. 201011020-4. We are very grateful also for the comments and contributions of anonymous reviewers and members of the editorial team.

References

Battha, L., 2004. Relative orientation with constraints for invariant geometric elements. Acta Geodaetica et Geophysica Hungarica 39 (1), 61–66.

Ha, J.E., 2009. Automatic detection of chessboard and its applications. Optical Engineering 48 (6), 067205(1-8).

Habib, A., 1999. Aerial triangulation using point and linear features. International Archives of the Photogrammetry and Remote Sensing 32 (Part 3-2W5), 137–141.

Habib, A., Kelley, D., 2001. Automatic relative orientation of large scale imagery over urban areas using modified iterated Hough transform. ISPRS Journal of Photogrammetry and Remote Sensing 56 (1), 29–41.

Habib, A., Morgan, M., Kim, E.M., Cheng, R., 2004. Linear features in photogrammetric activities. International Archives of Photogrammetry, Remote Sensing and Spatial Information Sciences 35 (Part B2/4), 610–616.

van den Heuvel, F.A., 1997. Exterior orientation using coplanar parallel lines. In: Proceedings of the 10th Scandinavian Conference on Image Analysis, Lappeenranta, Finland, 9–11 June, pp. 71–78.

van den Heuvel, F.A., 1998. Vanishing point detection for architectural photogrammetry. International Archives of Photogrammetry and Remote Sensing 32 (Part B5), 652–659.

Kubik, K., 1991. Relative and absolute orientation based on linear features. ISPRS Journal of Photogrammetry and Remote Sensing 46 (1), 199–204.

Laganière, R., Gilbert, S., Roth, G., 2006. Robust object pose estimation from feature-based stereo in instrumentation and measurement. IEEE Transactions on Instrumentation and Measurement 55 (4), 1270–1280.

Mikhail, E.M., Bethel, J.S., McGlone, J.C., 2001. Introduction to Modern Photogrammetry. John Wiley and Sons, Inc.

Nistér, D., 2004. An efficient solution to the five-point relative pose problem. IEEE Transactions on Pattern Analysis and Machine Intelligence 26 (6), 756–770.

Pan, H., 1999. A direct closed-form solution to general relative orientation of two stereo views. Digital Signal Processing 9 (3), 195–221.

Rahmann, S., Dikov, V., 2008. Relative pose estimation from two circles. Proceedings of the 30th DAGM Symposium on Pattern Recognition, Lecture Notes in Computer Science 5096, 375–384.

Schenk, T., 2004. From point-based to feature-based aerial triangulation. ISPRS Journal of Photogrammetry and Remote Sensing 58 (5–6), 315–329.

Smith, M., Park, D., 2000. Absolute and exterior orientation using linear features. International Archives of Photogrammetry and Remote Sensing 33 (Part B3), 850–857.

Stewénius, H., Engels, C., Nistér, D., 2006. Recent developments on direct relative orientation. ISPRS Journal of Photogrammetry and Remote Sensing 60 (4), 284–294.

Tang, L., Heipke, C., 1996. Automatic relative orientation of aerial images. Photogrammetric Engineering and Remote Sensing 62 (1), 47–55.

Tommaselli, A., Lugnani, J., 1988. An alternative mathematical model to collinearity equations using straight features. International Archives of Photogrammetry and Remote Sensing 27 (Part B3), 765–774.

Triggs, B., McLauchlan, P., Hartley, R., Fitzgibbon, A., 2000. Bundle adjustment – a modern synthesis. Vision Algorithms: Theory and Practice. Lecture Notes in Computer Science 1883, 298–372.

Wang, G.H., Wu, J., Ji, Z.Q., 2008. Single view based pose estimation from circle or parallel lines. Journal of Pattern Recognition Letters 29 (7), 977–985.

Warren, M., McKinnon, D., Gifford, T., Hu, H., Shiel M., Preller, D., Upcroft B., 2010. Vision only pose estimation and scene reconstruction on airborne platforms. In: Proceedings of Advanced Reasoning with Depth Cameras, Paper ID: 3, 27 June, Zaragoza, Spain (on CD-ROM).

Zhang, Z.X., Zhang, Y.J., Zhang, J.Q., 2008. Photogrammetric modeling of linear features with generalized point photogrammetry. Photogrammetric Engineering and Remote Sensing 74 (9), 1119–1129.

Zhang, Z.Y., 1998. Determining the epipolar geometry and its uncertainty: a review. International Journal of Computer Vision 27 (2), 161–198.